This article has been accepted for publication in IEEE Antennas and Wireless Propagation Letters. This is the author's version which has not been fully edited and content may change prior to final publication. Citation information: DOI 10.1109/LAWP.2025.3562934

Inverse Design Method of Antenna Based on Generative Artificial Intelligence

Quanhao Pang, Jun Ouyang, Feng Yang, *Member, IEEE,* Shiwen Yang, *Fellow, IEEE*, and Jun Hu, *Senior Member, IEEE*

***Abstract*—An antenna inverse design scheme based on generative artificial intelligence (AI) is proposed. The generative AI uses a diffusion model and incorporates a transformer model to output a series of innovative and practical antenna structures according to the input antenna requirements. To select the optimal structure from a large set of candidates, we further incorporate the Characteristic Mode Analysis (CMA) method into the Bilinear Convolutional Neural Networks (BCNN) model for evaluation and selection. The antenna inverse design scheme cleverly combines AI with the CMA method, which greatly simplifies the tedious process of traditional antenna design. By simply inputting the antenna requirements, the optimal antenna structure, distinct from existing datasets, can be rapidly obtained. Since the output is an antenna structure, it is not limited to a specific frequency band, thus offering design flexibility for cross-band adjustments. This letter presents case studies on single-band, dual-band, and wideband circularly polarized microstrip antennas to validate the practicality and effectiveness of the proposed scheme.**

***Index Terms*—Generative artificial intelligence, antenna inverse design, innovative antenna structure, characteristic mode analysis (CMA), bilinear convolutional neural networks (BCNN)**

I. Introduction

ANTENNAS, are crucial components in wireless communication systems, with their performance directly impacting overall system quality [1]. Currently, antenna design and optimization rely on electromagnetic simulation software, but this process is time-consuming and computationally intensive due to the need to consider numerous physical parameters [2]. As antenna designs grow more complex, human limitations become bottlenecks. Improving design efficiency and automating the optimal antenna design process is essential for advancing both technology and the wireless communication field.

In recent years, Machine Learning (ML) has great potential in the field of antenna performance prediction and antenna design[3]. Various ML algorithms, such as the K-Nearest Neighbors (KNN) [4]-[6], Support Vector Machines (SVM) [7]-[9], and Artificial Neural Networks (ANN) [10]-[12], have been employed to construct surrogate models that successfully predict antenna performance rapidly. The above studies can be considered as a forward optimization antenna process. Researchers have also made some progress in antenna inverse design[13]-[15]. However, these auxiliary methods have significant limitations. They are limited to optimizing antennas for a specific frequency band and cannot alter the basic antenna shape. Additionally, they cannot generate better designs or output structures outside the training dataset range. Most current neural network models focus on parametric electromagnetic modeling and optimization but fail to fully leverage the image generation capabilities of novel neural networks.

Generative AI techniques excel at capturing latent patterns in datasets to generate novel structures [16]. Common models include variational autoencoders (VAE), generative adversarial networks (GAN), and diffusion models. However, VAE-generated samples are often blurred or distorted, and GANs suffer from unstable training, leading to pattern collapse and low-quality, limited diversity in generated samples [17][18]. Diffusion models avoid these issues and allow flexible exploration of design possibilities beyond the training data constraints.

In this letter, we propose a generative AI framework for antenna inverse design to explore and develop superior antenna structures. The framework is based on a diffusion model. The model is able to generate antenna design structures not found in the datasets, which demonstrates a strong innovative ability and broadens the boundary of antenna design possibilities. Furthermore, we combine BCNN with CMA to classify and evaluate the diverse antenna structures generated by the diffusion model. The antenna inverse design scheme ultimately outputs the optimal antenna structure, which is not limited to a specific frequency band. It can flexibly incorporate the prior knowledge to adjust the antenna to any desired frequency band. To the best of the author's knowledge, this is the first time that generative AI has been applied to the field of antenna inverse design.

II. Introduction to Models and Antenna Inverse Design System

A. Principle of Diffusion Model

The Diffusion Model is a deep learning network for generative modeling [19]. In order to obtain the available antenna structures through the requirements of the input antenna, based on the traditional diffusion model, the encoder-decoder transformer architecture is used to

This work was supported in part by the Central Guidance on Local Science & Technology Development Foundation of Sichuan, China (Grant No. 2022ZYD0121); in part by the Foundation of Advanced Functional Composite Technology Key Laboratory of China (Grant No. 6142906220404); and in part by the Foundation of Sichuan Province Engineering Research Center for Broadband Microwave Circuit High Density Integration. (*corresponding author: Jun Ouyang, e-mail: yjou@uestc.edu.cn*)

The authors are with the School of Electronic Science and Engineering, University of Electronic Science and Technology of China (UESTC), Chengdu 611731, China (e-mail: 202311021813@std.uestc.edu.cn; yjou@uestc.edu.cn).

This article has been accepted for publication in IEEE Antennas and Wireless Propagation Letters. This is the author's version which has not been fully edited and content may change prior to final publication. Citation information: DOI 10.1109/LAWP.2025.3562934

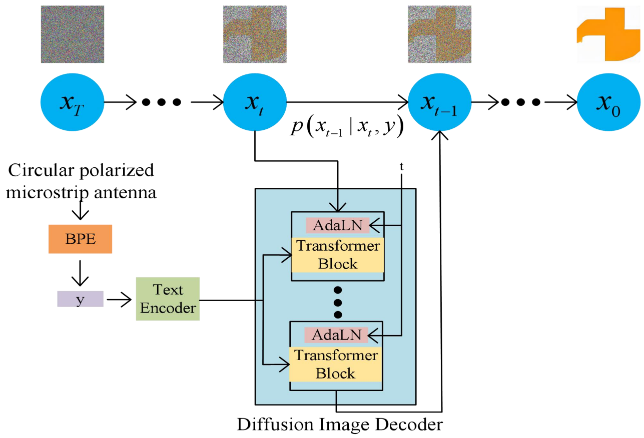

Fig. 1. The detailed schematic diagram of the diffusion model.

estimate the distribution $p(x_0 | x_t, y)$, where x_0 is the original noise-free image, x_t is a noisy image at a certain time step t in the diffusion process, y is the text mark obtained by BPE [20] encoding the input antenna requirements.

The entire diffusion model framework is shown in the fig. 1., including two parts: text encoder and diffusion image decoder. The text encoder is responsible for processing the input text tag y and generating a conditional feature sequence. This feature sequence serves as the conditional input for the diffusion image decoder, guiding image generation. The diffusion image decoder is the core part of the model. It receives the output of the noisy image x_t, the time step t, and the text encoder as the conditional input, and then outputs the distribution $p(x_0 | x_t, y)$ of the noise-free image. The diffusion image decoder consists of multiple Transformer blocks, each of which contains a self-attention mechanism and a feedforward network. The time step t is fed into the diffusion image decoder through the Adaptive Layer Normalization (AdaLN[21]) operator. These Transformer blocks can effectively understand and process text information, enabling the model to utilize the contextual information of the entire image, including both previously and currently predicted parts[22]. Finally, a Softmax layer converts the output of the Transformer block into a probability distribution, representing the likelihood of each image being noise-free. The loss function of the entire diffusion model framework is defined as follows

$$\begin{aligned} LOSS &= L_0 + L_1 + \cdots + L_{T-1} + L_T \\ L_0 &= -\log p(x_0 | x_1, y) \\ L_{t-1} &= D_{KL}(q(x_{t-1} | x_t, x_0) \| p(x_{t-1} | x_t, y)) \\ L_T &= D_{KL}(q(x_T | x_0) \| p(x_T)) \end{aligned} \tag{1}$$

D_{KL} represents the Kulback-Leibler (KL) divergence[23], which is a method to measure the difference between two probability distributions.

B. Principle of BCNN

BCNN is an effective architecture for fine-grained visual recognition, its schematic diagram is shown in Fig. 2. [24].The BCNN architecture is composed of four parts: two feature

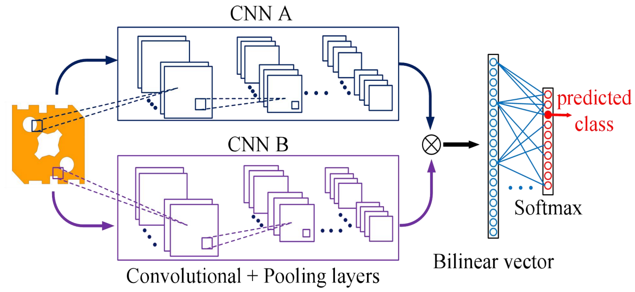

Fig. 2. BCNN schematic diagram.

functions (f_A and f_B based on CNN), a pooling function P and a classification function C . BCNN uses bilinear convolution to perform bilinear fusion operations on the features extracted by the two feature extraction networks to capture the interaction information between local feature pairs.

This method can model local features in a translation-invariant manner, thereby improving the sensitivity of the model to subtle differences in the image.

C. Antenna Inverse Design System Framework

The core components of the antenna inverse design framework consist of two parts: the diffusion model and the BCNN. The diffusion model takes the antenna design requirements as input. This process aims to innovatively generate a diverse set of antenna structures that do not exist in existing datasets. Then, all the generated antenna structures are screened and evaluated using the BCNN model incorporating CMA and the best performing antenna structure is selected. By simply taking the specific antenna requirements as input, the system can output the optimal antenna structure that meets the requirements. Subsequently, the CMA method can be further used to analyze the obtained antenna structure, adjustment of the resulting antenna structure to any desired frequency band, explore and determine the optimal feeding strategy[25], so as to complete the final closed-loop of antenna design and obtain the required antenna products.

III. Application Examples

In this section, we use three types of circularly polarized microstrip antennas as examples to verify the effectiveness of the inverse design system. We use a structural similarity comparison method that incorporates Structure Similarity Index Measure (SSIM) and Scale-invariant Feature Transform (SIFT) to calculate the similarity between the generated antenna structures and the antenna structures in the datasets. The experiment uses a single NVIDIA GeForce RTX 4060 Ti(16GB) to complete the training, and the training framework uses pytorch. The training period is 12 days, and the batch size is 4. The initial value of the learning rate is set to 1e-4.

After the framework training is completed, the accuracy of the inverse design system is verified. For each antenna type, 50 antenna structures are generated by the inverse design system, and their feasibility is evaluated using the CMA method. The final results are shown in Table I.

This article has been accepted for publication in IEEE Antennas and Wireless Propagation Letters. This is the author's version which has not been fully edited and content may change prior to final publication. Citation information: DOI 10.1109/LAWP.2025.3562934

TABLE I
ACCURACY OF THE INVERSE DESIGN SYSTEM

Antenna requirement	Structure obtained	Feasible Structure	Accuracy
CPMA	50	46	92%
DCPMA	50	45	90%
WCPMA	50	46	92%

CPMA, DCPMA, and WCPMA refer to the circularly polarized microstrip antenna, dual-band circularly polarized microstrip antenna, and wideband circularly polarized microstrip antenna.

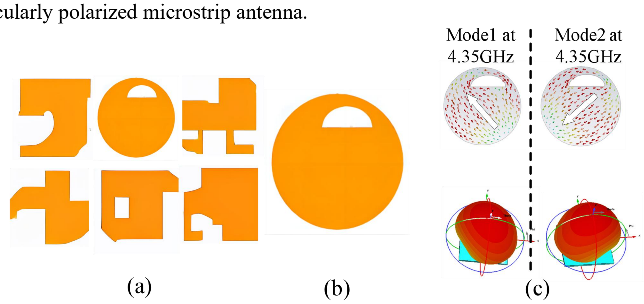

Fig. 3. (a) The structures generated by the diffusion model. (b) The Optimal Antenna Structure. (c) mode characteristics.

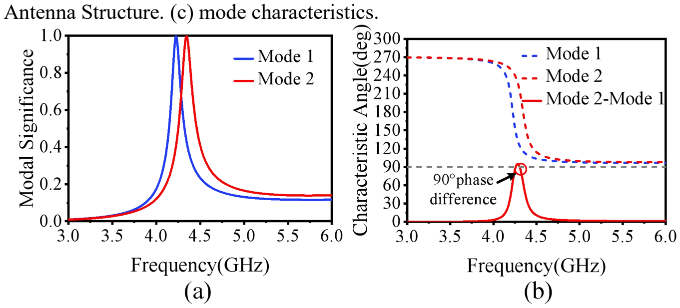

Fig. 4. (a) MS. (b) CA. The difference of CA between mode 2 and mode 1 is represented by Mode 2-Mode 1.

A. Circularly Polarized Microstrip Antenna

In this example, the antenna specific requirements are as follows: circularly polarized microstrip antenna.

The structures generated by the diffusion model and the final optimal structure are shown in Fig. 3. The optimal antenna structure is less similar to each antenna structure in the datasets with a maximum similarity of 64.59%. The results of CMA are shown in Fig. 3(c) and Fig. 4.

B. Dual-band Circularly Polarized Microstrip Antenna

In this case, the antenna specific requirements are as follows: dual-band circularly polarized microstrip antenna.

The structures generated by the diffusion model and the final optimal structure are shown in Fig. 5. The optimal antenna structure is less similar to each antenna structure in the datasets with a maximum similarity of 61.83%. The results of CMA are shown in Fig. 5(c) and Fig. 6.

C. Wideband Circularly Polarized Microstrip Antenna

In this example, the antenna specific requirements are as follows: wideband circularly polarized microstrip antenna.

The structures generated by the diffusion model and the final optimal structure are shown in Fig. 7. The optimal antenna structure is less similar to each antenna structure in the datasets with a maximum similarity of 62.87%. The results of CMA are

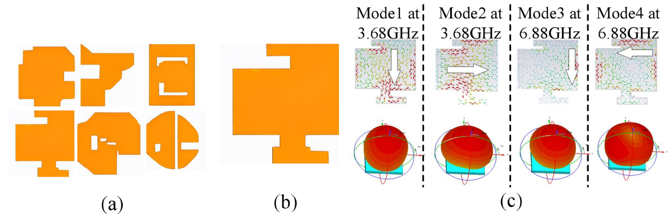

Fig. 5. (a) The structures generated by the diffusion model. (b) The Optimal Antenna Structure. (c) mode characteristics.

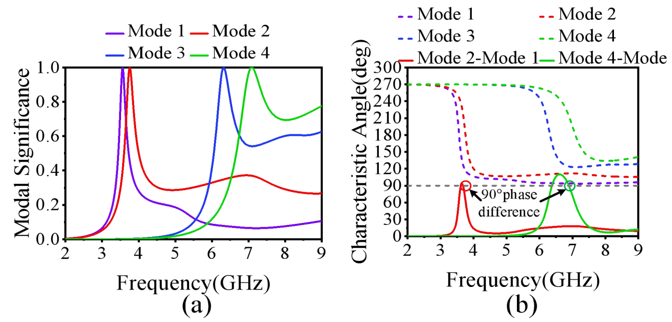

Fig. 6. (a) MS. (b) CA. The difference of CA between mode 2 and mode 1 is represented by Mode 2-Mode 1, and the difference of CA between mode 4 and mode 3 is represented by Mode 4-Mode 3.

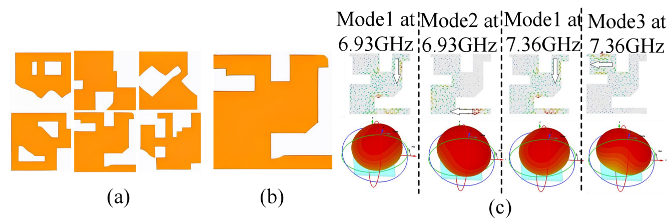

Fig. 7. (a) The structures generated by the diffusion model. (b) The Optimal Antenna Structure. (c) mode characteristics.

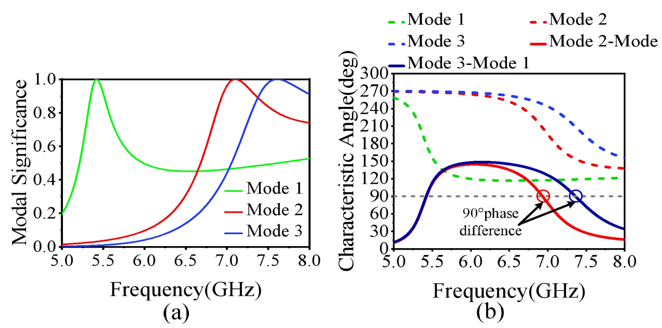

Fig. 8. (a) MS. (b) CA. The difference of CA between mode 2 and mode 1 is represented by Mode 2-Mode 1, and the difference of CA between mode 3 and mode 1 is represented by Mode 3-Mode 1.

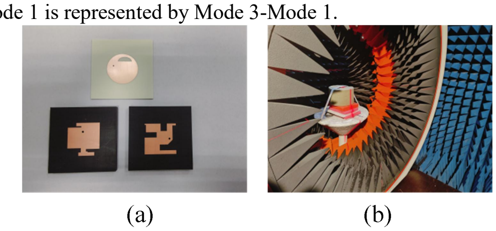

Fig. 9. (a)Fabricated antennas. (b)Measurement environment.

shown in Fig. 7(c) and Fig. 8.

IV. SIMULATION AND EXPERIMENTAL RESULTS

These three circularly polarized microstrip antennas are fabricated and measured, as shown in Fig. 9. Figs. 10-12

This article has been accepted for publication in IEEE Antennas and Wireless Propagation Letters. This is the author's version which has not been fully edited and content may change prior to final publication. Citation information: DOI 10.1109/LAWP.2025.3562934

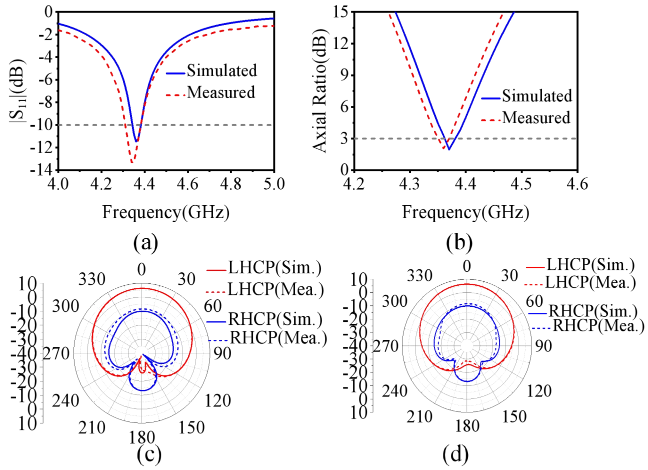

Fig. 10. Circularly polarized microstrip antenna simulated and measured results (a)S11. (b)AR. (c)xoz plane at 4.36 GHz (d)yoz plane at 4.36 GHz

TABLE II
COMPARISON OF ANTENNA

Ref.	Method	OSOD	Gain(dB)	Size(λ^3)
[26]	TM	\	5.8	$0.38\times0.38\times0.012$
[27]	TM	\	5.7	$0.27\times0.27\times0.01$
[28]	ML	No	4.51	$0.28\times0.28\times0.013$
Prop.	ML	Yes	6.26	$0.26\times0.26\times0.012$

TM represents traditional method. OSOD refers to the ability to output samples outside the datasets.

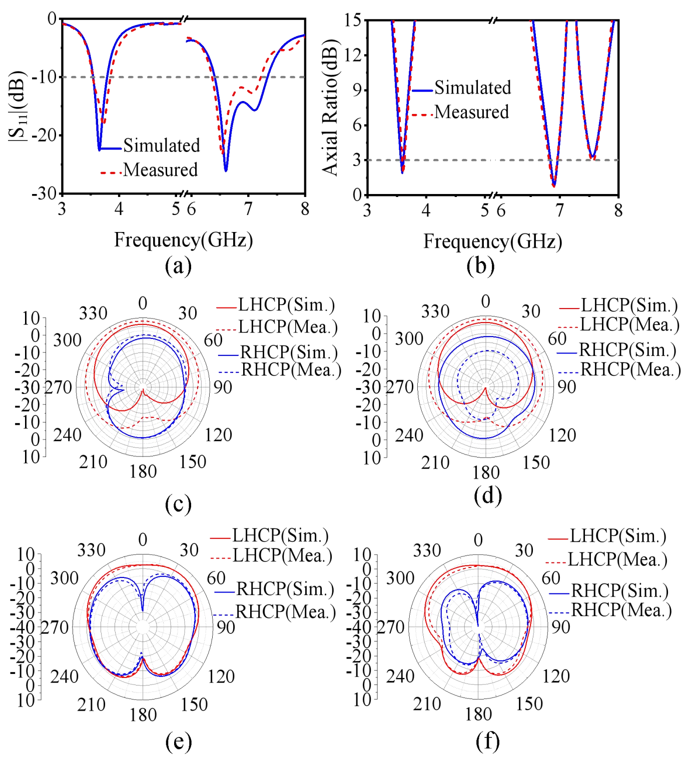

Fig. 11. Dual-band circularly polarized microstrip antenna simulated and measured results (a)S11. (b)AR. (c)xoz plane at 3.63 GHz (d)yoz plane at 3.63 GHz (e)xoz plane at 6.91 GHz (f)yoz plane at 6.91 GHz

show the simulated and measured results of the S11, AR, and radiation patterns of the three types of antennas, and the

TABLE III
COMPARISON OF ANTENNA

Ref.	Method	OSOD	Gain(dB)	Size(λ_1^3)
[29]	TM	\	6.10/4.96	$0.29\times0.25\times0.01$
[30]	ML	No	9.73/9.43	$0.35\times0.35\times0.028$
Prop.	ML	Yes	6.61/3.12	$0.23\times0.22\times0.018$

TM represents traditional method. OSOD refers to the ability to output samples outside the datasets. λ_1 Refers to the center operation frequency of the lower band.

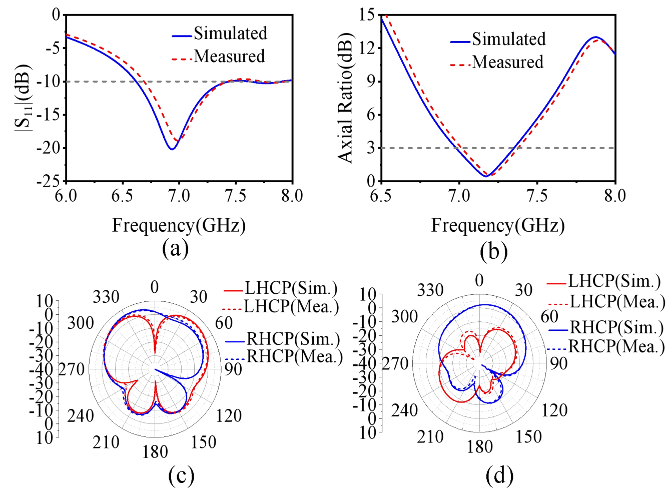

Fig.12. Wideband circularly polarized antenna simulated and measured results(a)S11.(b)AR.(c)xoz plane at 7.21 GHz(d)yoz plane at 7.21 GHz

TABLE IV
COMPARISON OF ANTENNA

Ref.	Method	OSOD	BW(S11/ AR)	Size(λ^3)
[31]	TM	\	7.7%/\	$0.53\times0.53\times0.035$
[32]	TM	\	5.4%/5%	$0.58\times0.56\times0.03$
[7]	ML	No	17.1%/\	$0.92\times0.92\times0.05$
Prop.	ML	Yes	12.8%/5.5%	$0.41\times0.41\times0.04$

TM represents traditional method. OSOD refers to the ability to output samples outside the datasets.

simulated and measured results are in good agreement. The comparisons with the previous works are shown in Table II-IV. The radiation direction of all antennas is $\theta = 0°$.

V. CONCLUSION

In this letter, an antenna inverse design framework based on generative artificial intelligence was proposed. The framework uses a diffusion model to generate novel antenna structures that differ from those in datasets. These structures are then evaluated using a BCNN model incorporating the CMA approach to identify the optimal antenna design solution. Notably, the inverse design system demonstrates a high success rate through a large number of example validations. More importantly, since the final output of this design framework is an antenna structure, it is not restricted to a specific antenna band, but can be flexibly adapted to the desired operating band, which demonstrates its excellent generalization capability.

REFERENCES

[1] Z. Chen et al., "Compact Wideband Circularly Polarized Loop Antenna Based on Dual Common and Differential Modes," *IEEE Antennas Wireless Propag. Lett.*, vol. 21, no. 8, pp. 1567-1571, Aug. 2022.

[2] A. Massa, D. Marcantonio, X. Chen, M. Li and M. Salucci, "DNNs as Applied to Electromagnetics, Antennas, and Propagation—A Review," *IEEE Antennas Wireless Propag. Lett.*, vol. 18, no. 11, pp. 2225-2229, Nov. 2019.

[3] D. Shi, C. Lian, K. Cui, Y. Chen and X. Liu, "An Intelligent Antenna Synthesis Method Based on Machine Learning," *IEEE Trans. Antennas Propag.*, vol. 70, no. 7, pp. 4965-4976, July 2022.

[4] B. Aspe et al., "Frequency-Tunable Slot-Loop Antenna Based on KNN Ferroelectric Interdigitated Varactors," *IEEE Antennas Wireless Propag. Lett.*, vol. 20, no. 8, pp. 1414-1418, Aug. 2021.

[5] L. Cui, Y. Zhang, R. Zhang and Q. H. Liu, "A Modified Efficient KNN Method for Antenna Optimization and Design,"*IEEE Trans. Antennas Propag.*, vol. 68, no. 10, pp. 6858-6866, Oct. 2020.

[6] Y. Sharma, H. H. Zhang and H. Xin, "Machine Learning Techniques for Optimizing Design of Double T-Shaped Monopole Antenna," *IEEE Trans. Antennas Propag.*, vol. 68, no. 7, pp. 5658-5663, July 2020.

[7] D. Shi, C. Lian, K. Cui, Y. Chen and X. Liu, "An Intelligent Antenna Synthesis Method Based on Machine Learning," *IEEE Trans. Antennas Propag.*, vol. 70, no. 7, pp. 4965-4976, July 2022.

[8] M. Tarkowski and L. Kulas, "RSS-Based DoA Estimation for ESPAR Antennas Using Support Vector Machine," *IEEE Antennas Wireless Propag. Lett.*, vol. 18, no. 4, pp. 561-565, April 2019.

[9] A. Motroni, M. R. Pino, G. Cecchi and P. Nepa, "A Near-Field Focused Array Antenna Empowered by Deep Learning for UHF-RFID Smart Gates," *IEEE Trans. Antennas Propag.*, vol. 71, no. 10, pp. 7946-7957, Oct. 2023.

[10] Y. He, J. Huang, W. Li, L. Zhang, S. -W. Wong and Z. N. Chen, "Hybrid Method of Artificial Neural Network and Simulated Annealing Algorithm for Optimizing Wideband Patch Antennas," *IEEE Trans. Antennas Propag.*, vol. 72, no. 1, pp. 944-949, Jan. 2024.

[11] J. Jin, Q. Su, Y. Xu, Z. He and Y. Lu, "Efficient Radiation Pattern Prediction of Array Antennas Based on Complex-Valued Graph Neural Networks," *IEEE Antennas Wireless Propag. Lett.*, vol. 21, no. 12, pp. 2467-2471, Dec. 2022.

[12] Y. Xiao, K. W. Leung, K. Lu and C. -S. Leung, "Mode Recognition of Rectangular Dielectric Resonator Antenna Using Artificial Neural Network,"*IEEE Trans. Antennas Propag.*, vol. 70, no. 7, pp. 5209-5216, July 2022.

[13] T. N. Kapetanakis, I. O. Vardiambasis, M. P. Ioannidou and A. Maras, "Neural Network Modeling for the Solution of the Inverse Loop Antenna Radiation Problem,"*IEEE Trans. Antennas Propag.*, vol. 66, no. 11, pp. 6283-6290, Nov. 2018.

[14] Y.-F. Liu, L. Peng and W. Shao, "An Efficient Knowledge-Based Artificial Neural Network for the Design of Circularly Polarized 3-D-Printed Lens Antenna," *IEEE Trans. Antennas Propag.*, vol. 70, no. 7, pp. 5007-5014, July 2022.

[15] S.Koziel and A. Bekasiewicz, "Rapid dimension scaling for notch frequency redesign of UWB band-notch antennas," *J. Electromagn. Waves Appl.*, vol. 30, no. 17, pp. 2280–2292, Nov. 2016.

[16] S. Bengesi, H. El-Sayed, M. K. Sarker, Y. Houkpati, J. Irungu and T. Oladunni, "Advancements in Generative AI: A Comprehensive Review of GANs, GPT, Autoencoders, Diffusion Model, and Transformers," *IEEE Access*, vol. 12, pp. 69812-69837, 2024.

[17] David Bau, Jun-Yan Zhu, Jonas Wulff, William Peebles, Hendrik Strobelt, Bolei Zhou, Antonio Torralba "Seeing What a GAN Cannot Generate", 2019 arXiv:1910.11626

[18] Soumik Mukhopadhyay, Matthew Gwilliam, Vatsal Agarwal, Namitha Padmanabhan, Archana Swaminathan, Srinidhi Hegde, Tianyi Zhou, Abhinav Shrivastava, "Diffusion Models Beat GANs on Image Classification", 2023 arXiv:2307.08702

[19] Jonathan Ho, Ajay Jain, Pieter Abbeel, "Denoising Diffusion Probabilistic Models", 2020 arXiv:2006.11239

[20] Rico Sennrich, Barry Haddow, and Alexandra Birch. "Neural machine translation of rare words with subword units", 2015 arXiv:1508.07909, 2015. 3

[21] Jimmy Lei Ba, Jamie Ryan Kiros, Geoffrey E. Hinton. "Layer normalization", 2016 arXiv:1607.06450,2016. 5

[22] Aditya Ramesh, Mikhail Pavlov, Gabriel Goh, Scott Gray, Chelsea Voss, Alec Radford, Mark Chen, Ilya Sutskever, "Zero-Shot Text-to-Image Generation", 2021 arXiv:2102.12092

[23] S. Kullback and R. A. Leibler, "On information and sufficiency", *Ann.Math. Statist*., vol. 22, no. 1, pp. 79–86, 1951.

[24] T. -Y. Lin, A. RoyChowdhury and S. Maji, "Bilinear CNN Models for Fine-Grained Visual Recognition," *2015 IEEE International Conference on Computer Vision (ICCV)*, Santiago, Chile, 2015, pp. 1449-1457.

[25] L. Y. Nie, B. K. Lau, S. Xiang, H. Aliakbari, B. Wang and X. Q. Lin, "Wideband Design of a Compact Monopole-Like Circular Patch Antenna Using Modal Analysis," *IEEE Antennas Wireless Propag. Lett.*,vol. 20, no. 6, pp. 918-922, June 2021.

[26] H. Liao and A. Shamim, "A Low-Profile and High-Aperture-Efficiency Hexagonal Circularly Polarized Microstrip Antenna Array," *IEEE Antennas Wireless Propag. Lett.*, vol. 21, no. 3, pp. 615-619, March 2022

[27] C. S. Lee, Y. Fan and M. Ezzat, "Single-Feed Circularly Polarized Microstrip Antenna With Bethe Holes on the Radiating Patch," *IEEE Trans. Antennas Propag.*, vol. 68, no. 6, pp. 4935-4938, June 2020

[28] L. -Y. Xiao, W. Shao, F. -L. Jin, B. -Z. Wang and Q. H. Liu, "Inverse Artificial Neural Network for Multiobjective Antenna Design," *IEEE Trans. Antennas Propag.*, vol. 69, no. 10, pp. 6651-6659, Oct. 2021

[29] D. Fazal and Q. U. Khan, "Dual-Band Dual-Polarized Patch Antenna Using Characteristic Mode Analysis,"*IEEE Trans. Antennas Propag.* , vol. 70, no. 3, pp. 2271-2276, March 2022

[30] A. Gupta, E. A. Karahan, C. Bhat, K. Sengupta and U. K. Khankhoje, "Tandem Neural Network Based Design of Multiband Antennas,"*IEEE Trans. Antennas Propag.* , vol. 71, no. 8, pp. 6308-6317, Aug. 2023,

[31] Y. -D. Yan, Y. -C. Jiao, H. -T. Cheng and C. Zhang, "A Low-Profile Dual-Circularly Polarized Wide-Axial-Ratio-Beamwidth Slot Patch Antenna With Six-Port Feeding Network," *IEEE Antennas Wireless Propag. Lett.*, vol. 20, no. 12, pp. 2486-2490, Dec. 2021

[32] N. -W. Liu, L. Zhu, Z. -X. Liu, G. Fu and Y. Liu, "Design Approach of a Single Circularly Polarized Patch Antenna With Enhanced AR-Bandwidth Under Triple-Mode Resonance," *IEEE Trans. Antennas Propag.*, vol. 68, no. 8, pp. 5827-5834, Aug. 2020